ANTIMICROBIAL NANOSTRUCTURED HYDROGEL WOUND DRESSING FOR THE TREATMENT OF CHRONIC WOUNDS

By

POOJA V. PATEL

A thesis submitted to the

School of Graduate Studies

Rutgers, The State University of New Jersey

In partial fulfilment of the requirements

For the degree offind

Master of Science

Graduate Program in Biomedical Engineering

Written under the direction of

Charles Roth, Ph.D.

And approved by

_____

_____

_____

_____

_____

New Brunswick, New Jersey

May, 2019

ABSTRACT OF THE THESIS

ANTIMICROBIAL NANOSTRUCTURED HYDROGEL WOUND DRESSING FOR THE TREATMENT OF CHRONIC WOUNDS

By POOJA PATEL

Thesis Director: Charles Roth, Ph.D.

Wound care is a substantial portion of the global market and treatment of chronic wounds cost the U.S. 25 million yearly on average. Bacterial biofilms are comprised of exopolymer encased bacterial cells and pose as a major health problem, as they are present in 78% of chronic, non-healing wounds. These biofilms frequently harbor multi-drug resistant microbial organisms (MRDOs) such as *Staphylococcus aureus*, *Pseudomonas aeruginosa*, and *Klebsiella pneumoniae*, which are difficult to eradicate with commercial antibiotics and greatly inhibit wound healing. Treatment is further complicated by poor blood circulation in the surrounding tissue, which hinders delivery of antibiotics to the infected region.

Our goal is to overcome the limitations of commercial antibiotics by developing a novel "GRAPLON Hydrogel" nanomedicine. The GRAPLON Hydrogel consists of unique graft polyelectrolyte surfactant (PS) nanocomplexes of cationic antimicrobial peptides (CAPs) which are known to minimize the development of microbial drug resistance. The PS-CAP nanoparticles (graft polyelectrolyte lipopeptide nanocomplexes or "GRAPLONs") are incorporated into a biopolymeric hydrogel that will function as a topical wound dressing. We hypothesize that the surfactant properties of the graft polyelectrolyte can cause physical disruption of biofilms and simultaneously enhance

transmembrane CAP delivery. In addition, the topical hydrogel can allow localized and controlled CAP delivery to the infected region, thereby reducing drug exposure and thus improving both efficacy and safety.

The physical properties of PS-CAP nanoparticles and GRAPLON hydrogels were characterized by measuring size, charge, surface tension, and viscosity. It was found that for specific graft density PS-CAPs, particle hydrodynamic sizes were <200 nanometers and were dependent on the solution they were dialyzed with. After complexing with CAPs Polymyxin B (PB) and experimental cyclic lipopeptides (CLPs), zeta potentials increased from negative to more positive, indicating self-assembling nanoparticle activity of the anionic polymer and cationic peptide through charge-charge interactions. Although critical micelle concentrations could not be determined, PS solutions did show presence of surface activity which was likely due to their graft density percentage. In hydrogel formulations, viscosities were demonstrated to be tunable based on addition of two different biocompatible thickening agents and shear thinning was observed due to the presence of CAPs and PS-CAPs. Controlled release studies demonstrated release kinetics in both aqueous and hydrogel formulations of PS-CAPs that closely fitted the Korsmeyer-Peppas kinetic model. Lastly, antibacterial activity was retained in in-vitro and in-vivo studies conducted on selected gram-positive and gram-negative bacterial biofilms. The cumulative results demonstrate great potential for the GRAPLON system to be an effective means of targeting bacterial biofilms in chronic wounds and providing a treatment that overcomes the current obstacles in this area of study.

ACKNOWLEDGEMENT

I would like to thank my advisors Dr. Charles Roth and Dr. Devore for giving me the opportunity and guidance to contribute to this study. I would also like to thank Ritu Goyal and Michael Holloway for being my lab mentors for the past years and the Rutgers Biomedical Engineering Department.

Additionally, a great thanks to Dr. Steve Davis University of Miami School of Medicine Department of Dermatology & Cutaneous Surgery and Dr. Richard Houghten at Torrey Pines Institute for Molecular Sciences and their respective lab groups for collaborative efforts.

This work is funded by the Department of Defense (DoD) Defense Medical Research and Development Program (DMRDP) Military Infectious Diseases Applied Research Award (MID-ARA) DM140052.

CONTENTS

LIST OF FIGURES

LIST OF TABLES

CHAPTER 1: INTRODUCTION

1.1 Clinical Significance

The clinical need for topical wound dressings for the treatment of chronic infections is becoming more prevalent. The wound care market is worth more than 6 billion globally and is expected to increase due to ongoing chronic conditions such as diabetes; 25 million goes into chronic wound care annually in the U.S. alone [1, 2].With the aging population and increased development of bacterial resistance, new methods to combat such obstacles need to be implemented in efficient and effective ways [1]. The market for wound healing is large and is still growing due to the need to treat chronic wounds that result from different conditions. Maintaining and caring for these wounds is tedious as well as expensive and is burdening for patients and medical personnel both. Chronic wounds are a result of when the wound healing process deviates from the norm due to internal factors like reduced metabolism and poor blood vasculature from preexisting diseases or external factors such as medications and infections. Different types of wound care dressings are used, such as gauze dressings. However, these types of dressings can be painful to remove because of their dryness and do not promote a moist environment. Other dressings are made from materials such as foam or semi-permeable gels that can be incorporated with antimicrobial substances or have antimicrobial properties themselves. In general, a good wound dressing should be easy to remove and replace, not stick to the wound, keep the wound moist, allow for air permeation and block out external debris such as bacteria. It should also minimize pain and cause the least amount of discomfort to the patient [3].

1.2 Bacterial Biofilms

Biofilms are a prevalent problem in a variety of settings, such as on the surfaces of industrial machinery, medical equipment and body surfaces [4]. Comprised of extracellular polymeric substances (EPS), biofilms can form over chronic, non-healing wounds caused through surgery, combat or burn injuries, in which they become considerably more difficult to heal, especially when the patient is older or has a compromised immune system [5]. The wounds can harbor different strains of bacteria such as *Staphylococcus aureus* and *Pseudomonas aeruginosa*, some of which have evolved to become multi-drug resistant organisms (MDROs). Thus, biofilms are particularly difficult to eradicate due to the combination of the resistant bacteria, external EPS film encasing, and poor blood circulation in the surrounding wound area. These issues highlight the need for a more effective chronic wound treatment solution.

Traditional treatments involve the use of high dose antimicrobial agents; however, such an approach contributes to the ongoing issue of bacterial resistance development [6]. The components of the EPS can also be targeted by removing essential nutrients that bacteria need to grow, but this may in turn harm the patient by depriving the wound area of factors needed to heal. Alternatively, the biofilm itself can be disrupted or detached, and the resulting break in that external barrier allows better exposure of the antimicrobial to the bacteria housed within. This lessens the need to create a more potent solution and offers a more controlled and targeted approach. Although the antimicrobial can be brought into the wound more effectively, it still faces the issue of being degraded rapidly within the body. To prevent this, a specialized carrier that protects while delivering the drug of interest would optimize the healing process and can provide treatment over a longer period.

1.3 Nanoparticle Delivery System

Nanoparticles (NPs) have emerged as a major class of drug carriers and have proven effective in targeted delivery and protection of sensitive cargoes from systematic degradation or fast clearance. While both liposomal and polymeric NPs are available, the latter tend to form more stable complexes with drugs and to have better controlled release properties [7]. They are further advantageous if they are biodegradable or biocompatible, which lowers the risk of further issues developing in the target site or the patient. Nanoparticles can be developed in numerous ways; in this study, the experimental peptides will be encapsulated by electrostatic self-assembly driven by polymer cationic-anionic interactions between the polymer backbone and peptides of interest.

Polyelectrolytes are a class of polymers that contain either a net positive or negative charge or a neutral charge due to ionized groups [8]. Because of these charged properties, polyelectrolytes are very soluble in water and are pH and temperature sensitive. Adjustable groups allow them to form complexes with other polyelectrolytes or charged molecules such as DNA or bioactive peptides, rendering them useful in their delivery in nanomedicine and gene therapy. Solubility in water eliminates the need to dissolve polyelectrolytes in harmful organic chemicals, binders or dissolving agents, thereby reducing potential toxic effects to patients in medical applications [9, 10]. Polyelectrolyte complexes can be formed in numerous methods; the most common is by mixing solutions of opposite charges gradually until complexes form [11], which can be then characterized by size and charge via dynamic light scattering (DLS) methods. There are many physiological barriers in drug delivery depending on the route of administration and target tissue, and many drugs are subject to rapid degradation [12, 13]. Drugs

complexed with polyelectrolytes have shown to be less prone to degradation and clearance and are also protected from serum molecule interactions, depending on how the complex is modified [14].

Combining polyelectrolytes or other polymer-based molecules with cationic peptides is shown to be an effective means of peptide delivery to the body, especially in areas that are difficult to reach or penetrate. Gao et al developed a block copolymer which was PEGylated at different lengths and grafted with cationic polypeptides. These were shown to retain their antimicrobial and antibiofilm properties against bacteria strains such as *P. aeruginosa* and *S. aureus*, reduced body adsorption and had low cytotoxicity in vitro [15]. Cationic peptides can also be encapsulated in nanoparticles. Almaaytah et al developed chitosan-based nanoparticles (CS-NPs) with an antimicrobial peptide RBRBR that demonstrated slow and linear release kinetics of the peptide from the nanoparticles. Additionally, the NPs caused a decrease in CFU's when tested against *S.aureus* strains, showed low toxicity, and had high inhibition of biofilm forming bacteria [16].

Hydrogels are becoming an increasingly utilized means of topical delivery of nanoparticles as they can allow controlled release of the formulation over the chronic wound and contain drug to remain primarily in the infected area [17, 18]. Use of NPs contained within a hydrogel matrix allows for a slower release of the drug, for example, preventing burst kinetics. A more gradual release is beneficial for a slow healing wound and prevents the drug from being cleared out by the body rapidly. In addition to being relatively fixed in place atop the wound, depending on its viscosity properties, a hydrogel can also keep the infected area moist and lessen discomfort to the patient. Unlike

traditional dressings which can cause pain when continually removed, especially for a wound that needs constant cleaning and redressing, hydrogels are less likely to bind or stick to the wound and make cleaning and reapplication easier [19]. Hydrogels can be formulated from synthetic materials like poly(ethylene glycol) (PEG) and PVA, or natural derived substances like alginate and chitosan [20]. Previous studies with hydrogels have shown that drug release is dependent on mesh size of cross-linked hydrogels and also on diffusion of the drug based on its size [21]. St'astny et al observed that hydrophobic drug release from HPMA-hydrogels is slow in release due to the controlled degradation of the hydrogel. It was also found that these hydrogels were more effective at doxorubicin (DOX) delivery than the free DOX [22]. In our study, biocompatible and non-toxic polysaccharide/cellulose based hydroxyethyl cellulose (HEC) and carboxyethyl cellulose (CMC) are used to form hydrogels with the polymer-peptide NPs. Both are water soluble and contain groups that make them pH responsive. Wen et al conducted a study forming hydrogels with HEC and CMC and tested for the release of bovine serum albumin (BSA) in different pH conditions. The amount of the BSA released depended on pH, suggesting the potential for such hydrogels to serve as a "smart" delivery system [23].

The polymeric nanoparticle-peptide complex combines all the desired features discussed above to create a novel hydrogel antimicrobial wound dressing. The polymer-peptide complex nanoparticles are dispersed in a biocompatible hydrogel matrix, as illustrated in Figure 1, and the particles can continually release in a controlled manner.

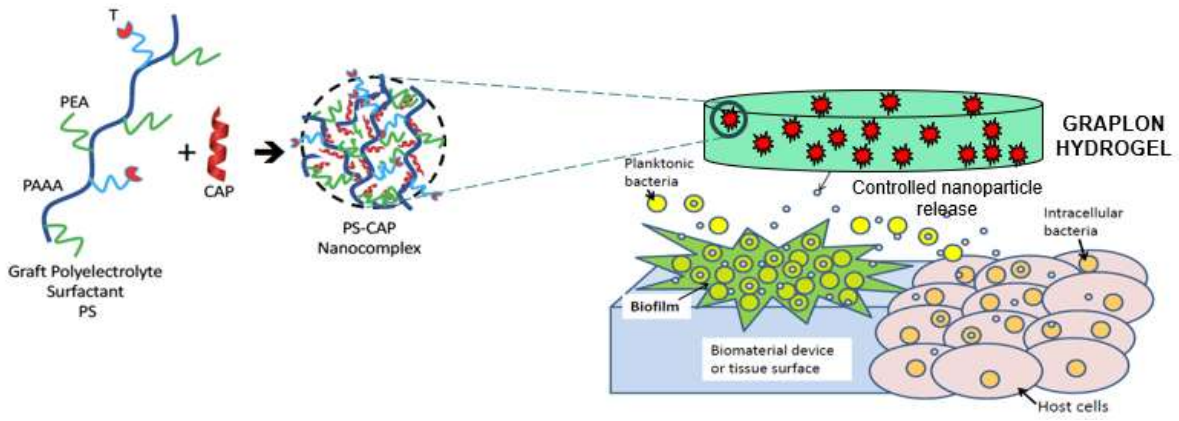

Figure 1: "GRAPLON" Nanoparticle Polymer-Peptide Hydrogel System Schematic

The GRAPLON hydrogel and its molecular components are characterized by size, charge, viscosity and surface tension measurements, properties of which demonstrate potential to be a viable topical treatment. We compare these property differences between different hydrogel formulations with combinations of graft copolymers and peptides. Additionally, the kinetics of drug release from the hydrogel are determined by controlled release experiments and its antimicrobial effectiveness are tested on bacterial biofilms through in-vitro and in-vivo studies.

CHAPTER 2: MATERIALS & METHODS

2.1 Formulation of Graft Copolymer and Peptide Complexes

2.1.1 Graft Copolymer Synthesis

The formulation begins with the synthesis of polymeric nanoparticles containing either a poly (methyl acrylic acid) (PMMA) or poly (propyl acrylic acid) (PPAA) backbone with covalently attached poly (ether amine) (Jeffamine M-2070) chains. The reaction is synthesized via carbodiimide coupling [24, 25]. PMMA acts as an anionic polyelectrolyte and since it can retain water, it makes it particularly useful in hydrogels. The graft PMMA is then complexed with the peptide of choice. The end solution is aqueous after graft polymer reconstitution and is dialyzed in a dialyzer cassette with either HPLC-grade water or 1X phosphate buffer saline (PBS). The amount of Jeffamine grafted was adjusted depending on the selected graft densities (1%, 5% and 10% Jeffamine). For this study, PMMA grafted with 10% Jeffamine, designated as PMMA-g-J10% is the primary polymer that the selected peptides are complexed with.

Synthesis Materials & Methods: PMMA (Polymer Source, Inc., Montreal, Quebec, CAN), anhydrous 1-hydroxybenzotriazole (HOBt) (Adv. Chem Tech., Louisville, KY), and Jeffamine M-2070 (Huntsman, The Woodlands, TX) were added to a nitrogen-flushed round bottom glass flask. After securing on a thermostatted magnetic stirrer, dry dimethylformamide (DMF) or tetrahydrofuran (THF) (Sigma Aldrich, St. Louis, MO) was added and contents were gently mixed a magnetic stir bar for 1.5 hours at room temperature until dissolved. Then, N, N′-diisopropylcarbodiimide (DIPC) (Sigma Aldrich) was added while reactants continued to stir. The temperature was raised to 50^{o}C and allowed to mix for approximately 30 hours. After mixing, the DMF or THF was

removed using a Rotary Evaporator. The resulting dried product in the flask was transferred to a larger flask, at which time 30 mL methanol (Fischer Chemical, Rockford, IL) was added and allowed to stir until the product dissolved. Then, 100 mL of diethyl ether (Fischer Chemical, Fair Lawn, NJ) was added very slowly (i.e. dropwise at a rate of 1 drop/2 seconds) to the methanol solution until the final polymer product precipitated. The precipitate was removed by filtering through a Buchner filter with a fritted disk and air dried for 1 hour. Then it was placed in vacuum for a final dry for 24 hours. Proton nuclear magnetic resonance analysis (H-NMR) was used to determine molecular weight. The carbodiimide coupling reaction is depicted in Figure 2.

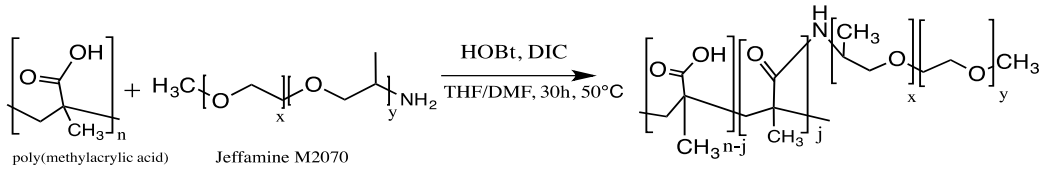

Figure 2: Synthesis reaction of Jeffamine M-2070 pendent chains grafted to PMAA backbone via carbodiimide coupling; reaction scheme derived from [25].

2.1.2 Complexing Graft Copolymers (PS) with Antimicrobial Peptides (CAPs)

The PMMA-g-Jeffamine polymer is then complexed with either commercially available standard antibacterial polymyxin B (PB) or experimental cyclic lipopeptides (CLPs) designated as 4 (CLP4) and 7 (CLP7), the latter which were synthesized and provided by Dr. Richard Houghten at Torrey Pines Institute for Molecular Studies. Polymyxin B is known to be effective against gram negative bacteria such as *P.aeruginosa* and *K.pneumoniae* and is water soluble [26]. As it is a cyclic molecule like the CLPs, it is used as a model compound in the studies. The CLPs are effective against

gram positive bacteria such as *S. aureus*; however, they are not soluble in water and require DMSO to dissolve. The amount of the graft copolymer required depends upon which percentage Jeffamine M-2070 is grafted onto the PMMA backbone to get the correct molar and charge ratios.

Materials and Methods for Polymer and Polymyxin B Complexes: PMMA-g-Jx% solid was weighed and added to 0.1 N NaOH (diluted from 10 M sodium hydroxide stock, Sigma Aldrich) solution in a glass screw gap vial to render a 4 mg/mL polymer solution. This was gently stirred with a small Teflon-coated stir bar at room temperature, covered with foil for ambient light protection, for 24 hours. The solution was removed and inserted into hydrated 10,000 MW Slide-A-Lyzer dialysis membrane cassettes (Thermo Scientific, Waltham, MA) in 2.5 mL aliquots with a syringe. The cassettes were then placed in individual 500 mL beakers filled with 200 mL of HPLC-grade water (Fischer Chemical), covered with parafilm and blocked from ambient light to start dialysis at room temperature. All 200 mL of HPLC water was removed and replaced with fresh HPLC water at 1, 3, 6, 24, and 30-hour time points. After 48 hours, the dialyzed solutions inside the cassettes were removed with a syringe, combined and placed in a new glass vial. The volume of the retained solution was measured by weighing the vial. The process was repeated but instead of using HPLC grade water for dialysis, 1X phosphate buffered saline, PBS, solution, was used instead. This rendered polymer solutions dialyzed with HPLC-grade water and 1X PBS.

Complexes with Polymyxin B: The next step was to form polymer-peptide complexes with the addition of 8.5 mg/mL Polymyxin B (PB) solution. The following method is described for PMMA-g-J10% (GP) with PB at a theoretical charge ratio of 0.563

(GP:PB). 8.5 mg/mL Polymyxin B sulfate salt (Sigma Aldrich) was prepared weighing PB in a glass screw cap vial and adding HPLC-grade water. This was vortexed until the PB solids dissolved completely, after which the solution was covered with foil until use. The 4 mg/mL dialyzed (HPLC or PBS) polymer solutions were sonicated for 20 minutes in an ice water bath at approximately 4^{o}C. An ice water bath was prepared in a beaker and a small Teflon-coated magnetic stirrer was added to a new glass screw cap vial. One mL of the sonicated polymer solution and 1 mL of HPLC water was added to the vial and the vial was placed in the beaker ice water bath mounted on a magnetic stir platform. Then, 0.80 mL of the 8.5 mg/mL PB solution was added dropwise (1 drop every 5 seconds) while the mixture was spinning over ice. This mixed for 10 minutes and then the final PMMA-g-J10%+PB solution was sonicated for 20 minutes in an ice bath. Afterwards, the solution was warmed to room temperature without any heat application and a 100 µL sample was removed and diluted 1:10 in HPLC water for size and zeta-potential analysis.

Complexes with CLPs: For cyclic lipopeptide solutions, the lipopeptides had to be dissolved in dimethyl sulfoxide (DMSO) (Fischer Bioreagents) due to their poor solubility. 50 µL of 8.5 mg/mL CLP (CLP4 and CLP7) dissolved in DMSO was combined with 50 µL of 5 mg/mL PS (PMMA-g-J10%) dissolved in DMSO in a vial and left to incubate at room temperature for 30 minutes. The combined 100 µL volume was then added dropwise (1 drop/5 seconds) into 0.9 mL of distilled water and mixed (self-assembly driven complexes). A small sample volume (50 µl) was removed and diluted for size and zeta potential analysis.

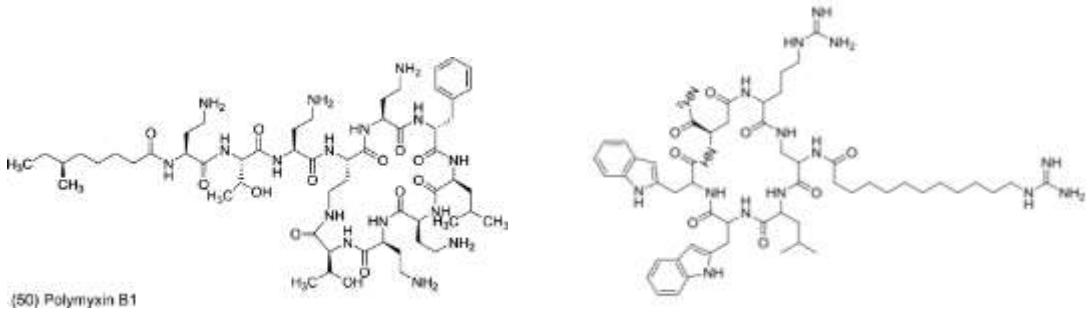

Figure 3: Structures of Polymyxin B, left [26] and novel fusaricidins (cyclic lipopeptides - CLPs), right; both are cyclic molecules.

2.1.3 Hydrogel Formulation

The graft copolymer and peptide complex aqueous solution is made into a hydrogel solution by the addition of hydroxyethyl cellulose (HEC) or carboxymethyl cellulose (CMC) dry powder, both of which substances are biocompatible thickening agents. The amount added was adjusted so that the final hydrogel was viscous enough to stay in place but still fluid enough so that the hydrogel could be removed and replaced easily.

Hydrogel Sample Preparation: For both HEC and CMC samples, aqueous solutions of PMMA-g-J10%+PB, PMMA-g-J10%+CLP were prepared by the addition of HEC and CMC by 2%, 3%, and 5% weight/volume (w/v). Approximately 2 mL of aqueous solutions were prepared for each in 15-mL conical plastic tubes. For CMC hydrogels, dry CMC powder (Sigma Aldrich) was weighed and added, and the solution was vortexed briefly until it became viscous and was set at room temperature. For HEC hydrogels, dry HEC powder (Tokyo Chemical Industry America, Portland, OR) was weighed and added, and the solution was vortexed briefly until the HEC was fully hydrated. It was rested at room temperature for 30 minutes and then vortexed again until the solution became viscous. Controls for the PMMA-g-J10% only and CLP only were not made due to

limited working material. All samples were rested at room temperature for 1 hour or more before viscosity measurements were taken.

2.2 Physicochemical and Mechanical Characterization of Aqueous and Hydrogel Formulations

The size (hydrodynamic diameter in nanometer) and zeta potential (ZP in millivolts) of the different graft polymer and peptide complexes are analyzed to determine surface charge properties, stability, and appropriate size that falls within what is considered nanoparticle range (<200 nanometers) and surface charge (ZP) that corresponds to the theoretical charge ratios and anionic/cationic properties of the molecules.

2.2.1 Hydrodynamic Particle Diameter Size in Aqueous Solutions

Size of the nanoparticle system is important as it determines the overall stability of the complex and how well it can deliver the peptide into an infected wound. For nanoparticles, the size should preferably not exceed 200 nanometers. Particle hydrodynamic diameter was determined using digital light scattering methods (DLS) using Malvern Zetasizer Nano ZS90 (Malvern Instruments, UK). Reconstituted polymer-peptide complex solution samples, after 20-minute sonication in an ice bath, were diluted 1:10 in distilled water and measured immediately after with input parameters: refractive index of PMMA (n = 1.49) [27] at 37^{o}C with 120 second equilibration time in a reusable Zetasizer DTS cuvette. Data analysis was performed automatically, and size was averaged over an optimized number of runs (>100 runs). Instrument algorithms are based on Brownian motion correlation to estimate particle size [25, 28].

2.2.2 Zeta Potential

Along with size, surface properties of the nanoparticles are equally important as they can determine the hydrophilicity and be predictive of the NPs interaction with other molecules in the body. Measuring the zeta potential gives a good metric for these surface interactions and are indicative of proper complexing from charge-charge interactions. Zeta potential is determined along with size in the Malvern Zetasizer Nano ZS90 instrument and the sample is also diluted 1:10 in distilled water, refractive index of PMMA (n = 1.49) at 37^{o}C with 120 second equilibration time. Likewise, data analysis was performed automatically, and zeta potential was determined from the average of an optimized number of runs (>100 runs).

2.2.3 Surface Activity

An additional physical surface property of interest is the surface tension of the graft polymer solutions without the added peptide. The surface activity of the polymers is an important factor in their homotypic self-assembly, their interaction with a cargo such as CAPs, and the interactions with biological structures. For example, the presence of surfactant-like properties of the NP solutions has been associated with less interaction with molecules within the body and therefore less uptake and clearance of the complexes internally [29]. Sample solutions were measured with a Fisher Surface Tensiomat Model 21 (Fischer Scientific, Dubuque, IA) using the surface balance ring method at room temperature over a range of concentrations, as both the slopes governing the decrease in surface tension with polymer concentration as well as the critical micelle concentration (CMC) are of interest. Samples were prepared by making a highly concentrated stock

solution as possible for each substance to be measured, which was then used to make dilutions with HPLC-grade water at a logarithmic range and measured accordingly in triplicate. In addition to the graft polymer solutions, the surface tensions of the un-grafted polymers PMMA and PPAA, Jeffamine M-2070, and standard surfactants polysorbate-20 (Tween 20) (Acros Organics/Thermo Fischer Scientific, Waltham, MA) and Triton X-100 (Promega, Madison, WI) were measured as well for comparison.

Dunouy Ring Balance Methods: Approximately 4 -5 mL of each sample at each concentration was needed for proper measurement. The titanium Dunouy ring was cleaned by holding in a flame of a Bunsen burner with metal tweezers until glowing red and hung on the tensiometer hook to cool. The sample was filled in a plastic, 3.5 cm tissue culture well plate (glass containers can also be used, but due to small working volume, this vessel was selected) with a 5-mL serological pipette. The plate was placed under the hung ring and the bottom lever was raised until the ring was submerged right below the surface of the sample. The Vernier caliper measurement knobs were adjusted until the ring was pulling at the surface of the sample. Once the balance was properly aligned and on level with the indicated line on the balance, the caliper was very slowly rotated until the ring pulled out of the sample surface. The moment this occurs is what is measured as the surface tension, as indicated by the caliper by 2 significant figures. This is repeated for the same sample thrice and the resulting values are averaged to get the surface tension.

2.2.4 Rheological Properties of Hydrogels

Viscosity of the prepared hydrogels are important in making sure that the hydrogel formulation is viscous enough to stay in place during formation and administration but also fluid enough to allow controlled release of the NPs. Additionally, the changes in viscosity due to peptide addition or no peptide addition can also be observed via shear thinning behavior. Viscosity was measured with the Malvern Kinexus Rheometer (Malvern Instruments, UK) at 20^{o}C using a linear shear rate ramp method on rSpace software to determine the shear viscosity at specific shear rates (s^{-1}) over an interval range from 0.1 to 100 with 10 samples for 5 minutes. Working gap length was set at 0.6 mm and PU20 SC0044 SS/PL65 S0380 SS parallel plate top/bottom geometry was used. Approximately 1 mL sample of hydrogel formulation was dispensed on rheometer with a disposable plastic dropper, properly trimmed and subjected to the automated ramp test. Samples formulated with guar gum were also tested, however experiments were discontinued as they were prone to fungal contamination as a result of being left at room temperature.

2.3 Controlled Release, In-vivo and In-vitro Studies

2.3.1 Controlled Release Profiles

Controlled release profiles of the peptide release from the aqueous solution compared to that released from the hydrogel formulation is important in order to determine how effectively the peptide is released from both solutions. Release rate of the peptide is critical to its bioavailability in circulation and its potential to be effective on chronic wounds which require longer times to heal.

Controlled release profiles were obtained by injecting with a syringe approximately 1 milliliter each of aqueous and hydrogel (2% HEC) solutions of PMMA-g-J10%+PB in separate dialysis cassettes of MW 10,000 (Slide-A-Lyzer Dialysis Cassettes, Thermo Scientific, Waltham, MA). The cassettes were then placed in beakers filled with 150 mL of 1X PBS and the beakers were then placed in a 37ºC shaking water bath and covered with parafilm. Samples were taken from the PBS solution by removal and replacement of 5 mL PBS (to maintain total volume in the beaker) at 0, 0.5, 1, 6, 24, and 114 hours. The amount of peptide released into each sample was measured using HPLC methods described below. Dilutions of Polymyxin B were prepared to use as standard solutions to estimate how much was released into the samples. A stock solution of 4.25 mg/mL PB was prepared and serially diluted 1:1 to 0.125 mg/mL (6 dilutions total: 4.25, 2.120, 1.060, 0.503, 0.251, 0.125 mg/mL).

HPLC Methods: The Waters 2695 Separations Module, Waters 2489 UV/Visible Detector was used along with Empower software. 0.5 mL of samples from aqueous solutions, hydrogel solutions, and PB dilutions were pipetted into HPLC vials and loaded into the HPLC. Water blanks were also included with these and were added in the beginning, middle, and end of the vial sequence. A Symmetry Shield RP18 Analytical Column was inserted. Condition parameters were as follows: 25ºC temperature, 10 microliter injection volume, 0.5 mL/min flow rate and 6-minute run time at a detection wavelength of 215 nm. The two mobile phases were A: HPLC water and B: acetonitrile, both with 0.1% trifluoroacetic acid. Resulting controlled release data was plotted and fitted with 4 release kinetics models (Zero order, first order, Higuchi, and Korsmeyer-Peppas) [30, 31].

2.3.2 In-Vitro Bacterial Minimum Inhibitory Concentration (MIC) and Minimum Biofilm Eradication Concentration (MBEC) Assays

Selected strains of bacteria were used to perform bacterial assays to determine minimum inhibitory concentrations (MICs), which is the minimum concentration of solution needed to eliminate bacteria growth. Bacteria were prepared at an optical density (OD) of 600 and 100 µL of bacteria of $1x10^6$ cells/mL in tryptic soy broth medium (TSB – 30 g/L and autoclaved at 121^{o}C for 15 minutes) (BBL Trypticase Soy Broth, Becton, Dickinson, and Co., Sparks, MD) were pipetted into the interior rows of a 96-well plate (avoiding wells on the borders of plate). Stock solutions of peptides of selected concentrations were prepared in TSB and 200 microliters of these solutions were pipetted into the first column (B2 to G2) in a separate 96-well plate. 100 µL of TSB medium was added to the remaining wells (9 columns) of this plate. 1:1 serial dilution was made in the wells by using a multi-channel pipette to take out 100 µL from the first column and add dispense in the next row, thoroughly mix and repeat in the next 8 columns. After the 100 µL each dilutions of peptide were prepared, these were transferred to the bacteria plate for a total volume of 200 µL in each well.

The minimum biofilm eradication concentrations (MBECS) were also obtained using a high-throughput polystyrene microtiter 96-well plate assay. Biofilms were grown by adding $1x10^6$ CFU/TSB in each well and incubating for 48 hours at 37^{o}C. Biofilms were then washed with PBS twice and dilutions of PS-peptides solutions were added. Plates were incubated for 24 hours, washed with PBS twice and 100 µL of 10%

alamarBlue reagent (Thermo Fisher Scientific) was added. Absorbances were measured at 560 nm with a microplate reader.

2.3.3 Porcine Wound In-vivo Pilot Study

A pilot study conducted at University of Miami used porcine wounds infected with MRSA to test the polymer hydrogel formulations with the novel cyclic lipopeptides (CLPs) developed at the Torrey Pines Institute for Molecular Studies. 5 mL each of 7 mg/mL (CLP/mL) PS-CLP4 AND PS-CLP7 were prepared and divided into 1-mL calibrated glass syringes and shipped for the study. The hydrogels were formulated with 2% HEC. Additionally, a control hydrogel containing only PS and CLP in DMSO solution were also prepared and sent. The partial thickness wound study methods were derived from previously established methods conducted by the group [32]. Two female pigs were used and were kept under controlled feeding, temperature, and light/dark cycle conditions and followed all federal guidelines for containment and care for laboratory animals. Partial thickness wounds (10mm x 7mm x 0.3mm) were made on the skin surface with an electro keratome and were kept 15 mm apart. Wounds were infected with 25 microliters of 10^6 CFU/mL MRSA USA300 and treated with 100 µL of each treatment once daily for 5 days. 2% mupirocin was used as positive control and an untreated control wound was left as well. After treatments (4 wounds per treatment), wounds were covered with polyurethane film dressing to promote biofilm formation and prevent cross contamination. At days 2 and 5, bacteria samples were collected with a

sterile spatula from the designated wounds and collected in 1 mL PBS for bacteria viability studies [33].

CHAPTER 3: RESULTS & DISCUSSION

GRAPLON + Peptide Physical Characteristics: Upon forming the polymer-peptide complexes, the solutions for each of the three complexes with graft densities of 1%, 5%, and 10% Jeffamine (designated PMMA-g-Jx%) were clear with a slight blueish tint. Both polymer solutions and PB solutions were clear with no tint before slow addition of PB solution to the PMMA-g-Jx% solutions. The slight tint without presence of turbidity or precipitate is a visual indicator that nanocomplexes have self-assembled.

The stability of polymers themselves and of polymer-peptide complexes was investigated. Table 1 below lists initial ZP and sizes of graft polymers complexed with PB prepared and measured in 2016. It is seen in Table 1 that even after 2 weeks post preparation, particle sizes start to increase slightly. A Student's t-test was performed for the initial samples and post two-week samples and the difference between the means were significant for PMMAgJ1%+PB and PMMAgJ5%+PB samples ($p = 0.0468$, $p = 0.04332$; $p < 0.05$) and not significant for PMMAgJ10%+PB ($p = 0.1228$; $p > 0.05$).

	Initial		**Post 2-week preparation**	
Sample	Zeta Potential (mV)	Size (nm)	Zeta Potential (mV)	Size (nm)
PMAA	-37.5 ± 3.9	-	-	-
PMMAgJ1%	-15.1 ± 1.06	-	-	-
PMMAgJ5%	-20 ± 1.1	-	-	-
PMMAgJ10%	-31.2 ± 1.3	-	-	-
PMMAgJ1%+PB	-17.4 ± 2.5	71.9 ± 2.1	-14.5 ± 4.8	86.5 ± 2.5
PMMAgJ5%+PB	-9.7 ± 0.8	53.7 ± 0.1	-17.8 ± 3.4	56.7 ± 0.6
PMMAgJ10%+PB	0 ± 0.06	39.6 ± 0.6	-0.4 ± 0.1	44.6 ± 1.9

Table 1: Summary table of hydrodynamic diameter sizes of particles and respective zeta potentials; Polymer solutions prepared in distilled water (CR = 0.5, N = 3; measurements taken Oct. – Nov. 2016).

Resized PS-PB complexes made from four-month-old PS stocks preparations shows an increase in zeta potentials after complexing polymers with PB, indicating charge-charge interactions (Table 2). The 10% graft density samples are more stable in terms of size and lower polydispersity indexes in the PMMAgJ10% PB complexes, even though sizes are >100 nm. Although sizes of the graft polymer only are highly variable and of low quality, the polymer-peptide complexes made from the polymer only solutions produce smaller and more homogeneous particle sizes in the polymer-peptide solutions. Table 3 summarizes ZP and size data from PS-PB complex solutions measured within 24 hours of when the complexes were made. These sizes are significantly smaller than those in Table 2 even though they are made from the same stock polymer solutions and were also sonicated before measuring. We can conclude that over time, solutions start to aggregate in a manner that may be dependent on the graft density of the polymer.

Sample	Zeta Potential (mV)	Hydrodynamic Diameter (nm)	Polydispersity Index
PMMAg10% HPLC*	-53.1 ± 3.1	465.8 ± 196.5	0.84
PMMAg10% PBS*	-23.4 ± 1.3	279.4 ± 168.2	0.52
PMMAg10%+PB HPLC	4.5 ± 0.4	243.7 ± 6.7	0.39
PMMAg10%+PB PBS	-18.7 ± 0.3	142 ± 2.3	0.22
PMMAg5% HPLC*	-30.1± 5	305.5 ± 42	0.51
PMMAg5% PBS*	-28.4 ± 1.2	133.1 ± 17.1	0.8
PMMAg5%+PB HPLC	3 ± 0.1	374 ± 10.4	0.45
PMMAg5%+PB PBS	-1.1 ± 0.1	953 ± 26	0.49
PMMAg1% HPLC*	-28.8 ± 4.4	791.3 ± 279.6	0.53
PMMAg1% PBS*	-57.3 ± 1.6	610.8 ± 6.4	0.4
PMMAg1%+PB HPLC*	14.2 ± 0.4	2115.7 ± 146.4	0.76
PMMAg1%+PB PBS*	2.6 ± 0.3	874.3 ± 187.8	0.45
Polymyxin B	7.7 ± 2.0	318.5 ± 5.2	0.28
PMAA only	-12.3 ± 0.6	26 ± 1.1	0.68

Table 2: Summary table of zeta potentials, particle diameter sizes and polydispersity indexes of polymer and polymer-peptide solutions made from four month-old stock polymer solutions using DLS (CR = 0.5 for all PS-PB solutions, N = 3; measurements taken Mar. 2019).*Indicates data of low "quality factor" due to multiple scattering, large

population, and flare issues largely due to aggregation or sedimentation occurring in sample.

Table 3 summarizes the particle hydrodynamic diameter size (nm) and zeta potentials (mV) for the three graft-density polymers complexed with PB (2018 measurements) and measured within 24 hours of preparation. Polymer solutions were dialyzed with either HPLC-grade water or 1X PBS as it was expected that the presence of salt would affect and the size and charge through screening of electrostatic interactions. For the 5% and 10% graft densities, particle sizes are lower by almost half in the PBS dialyzed solutions when compared to the water solutions. Zeta potentials (ZP) are also both in the negative range for those as well. For all three graft densities, the water zeta potentials are greater (more cationic) than the corresponding PBS zeta potentials. For the 1% grafted complex, both the PBS and water dialyzed solutions are >>200 nm. The solution was visibly opaque and had some slight precipitate. It may be that 1% has in insufficient level of grafting to impart stability to complexes of PB with PMMA family polymers.

The initial size measurements from 2016 (Table 1) are far smaller than the those measured in 2018 and 2019 (Table 2, 3); nonetheless the 2019 measurements in indicate that older polymers can be reconstituted and still form sub-micron particle sizes. The sizes in Table 3 are significantly smaller than those in Table 2 even though they are made from the same stock polymer solutions and were also sonicated before measuring. We can conclude that over time, solutions start to aggregate in a manner that may be dependent on the graft density of the polymer.

	Water Dialyzed			PBS Dialyzed		
Sample	Zeta Potential (mV)	Size (nm)	Polydispersity Index	Zeta Potential (mV)	Size (nm)	Polydispersity Index
PMMAgJ1%+PB	+13.0	1023*	0.386	+6.4	2030*	0.881
PMMAgJ5%+PB	+4.7	224	0.175	-2.7	129	0.056
PMMAgJ10%+PB	+3.0	130	0.2	-10.3	76	0.132

Table 3: Summary table of hydrodynamic diameter sizes of particles and respective zeta potentials of polymer-PB complexes, and polydispersity indexes, all measured simultaneously using DLS (CR = 0.5 for all PS-PB solutions, N = 1; measurements taken Oct. – Nov. 2018). *Indicates size data of low "quality factor" due to aggregation/sedimentation within sample.

Figure 4 shows particle diameter size intensity distribution plots that correspond with size data from Table 3. For all plots, the peaks are strongest at the calculated average size with very low small populations of particles of other sizes in PMMA-g-J10%+ PB's size distribution. Singular, strong peaks indicate good quality of data and a relatively homogenous population of particles. Data can also be deemed of good quality for the 5% and 10% solutions based on the polydispersity indexes.

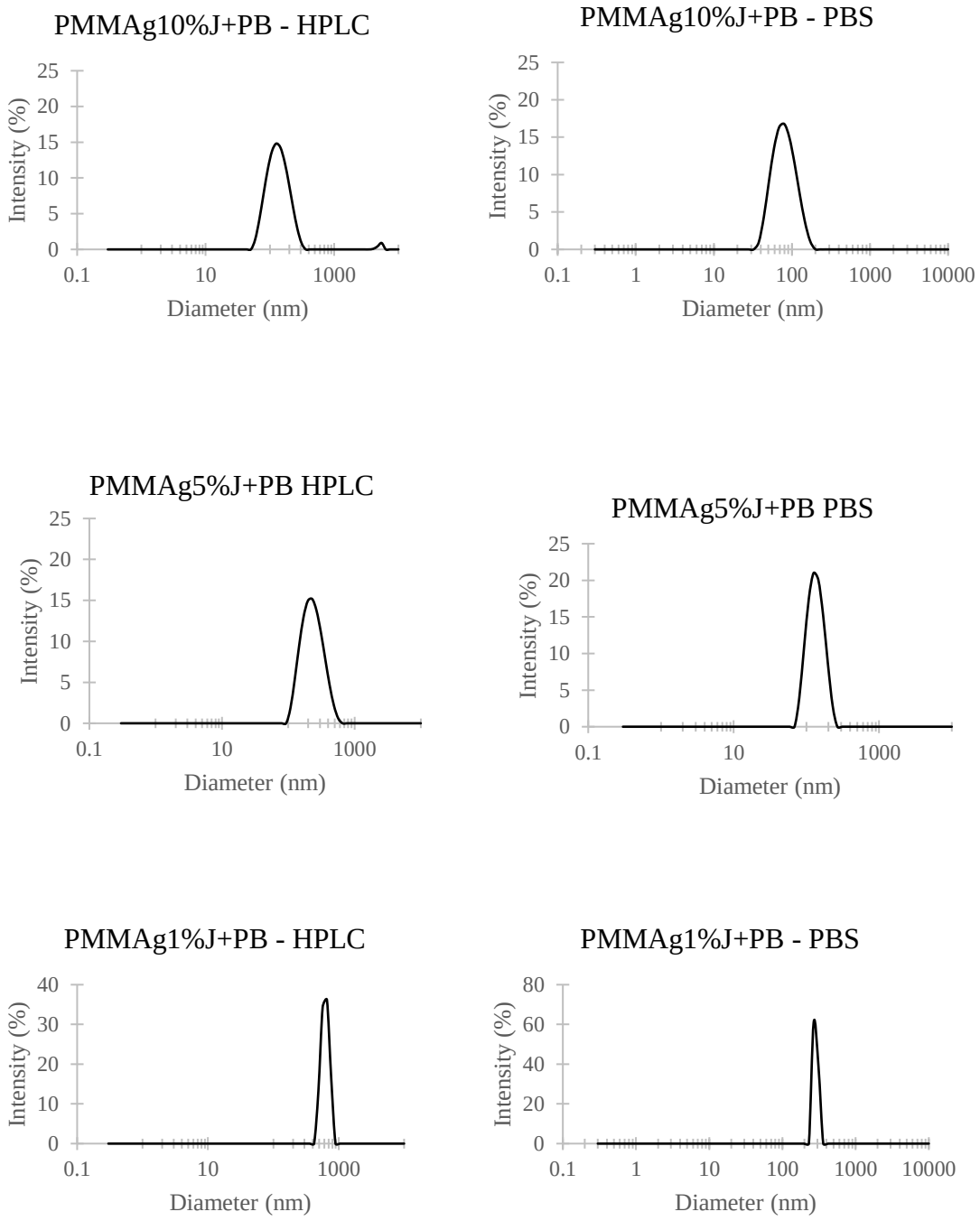

Figure 4: Particle hydrodynamic diameter size distribution plots showing average particle size and intensity. Peaks indicate strongest signal measured in intensity for the indicated diameter.

The above plots in Figure 4 are a cumulant fit from correlation curves, which is how the diffusion coefficient is acquired, which in turn is used to estimate particle size (hydrodynamic radius). The average value, or z-average, is weighted by the particle scattering intensity. If a sample is of good quality, i.e. particle sizes are homogeneous, the graph will produce a singular peak and the correlogram has a single decay [34]. In the case of the PMMA-g-J1% samples, the z-average is obtained as >1000 nm for both HPLC and PBS even though the intensity graph displays peaks below 1000 nm. This is likely because of aggregates or sedimentation occurring in the sample, creating some particles well over the instrument measurement range (0.6 nm to 6 microns) and the instrument attempting to fit the large particle size in the data. The large particle size and polydispersity is also indicated in the below correlograms (Figure 5). For both PBS and HPLC samples, the correlogram for PMMA-g-J1%+PB solutions (blue) decays at later times and exhibits multiple decays, indicating multiple populations each of large size. Size data outputted are not reliable for this 1% graft density polymer sample set.

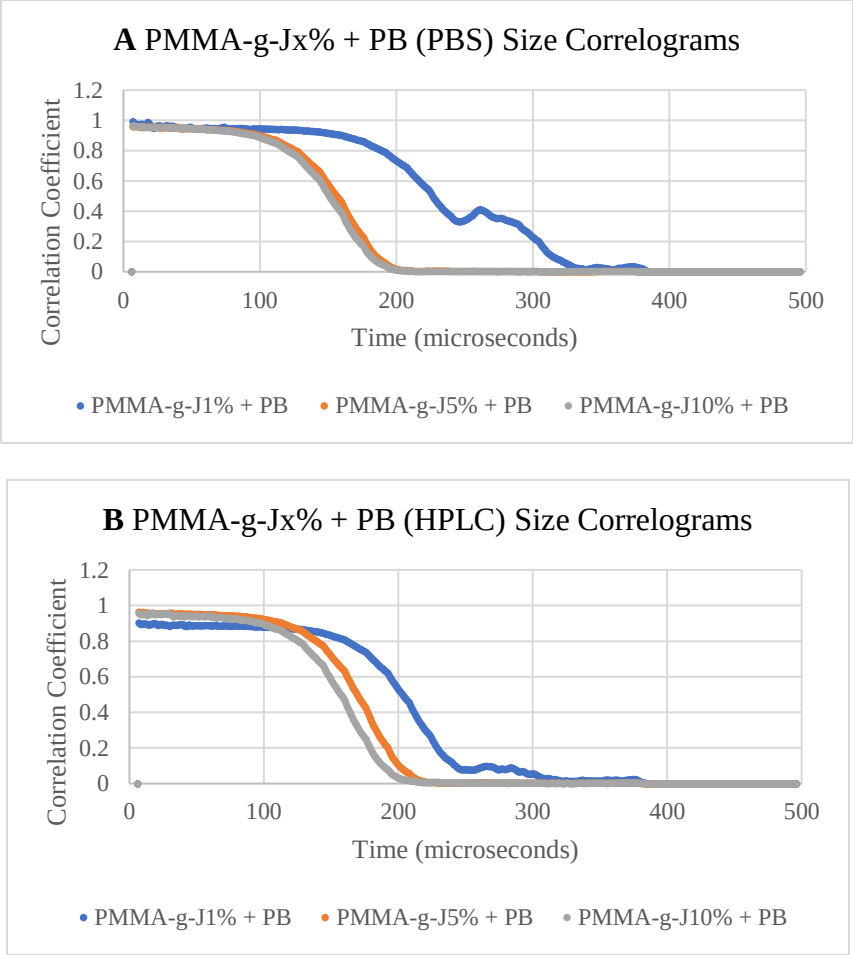

Figure 5: A, B – Correlograms for PMMA-g-Jx% + PB complexes dialyzed in HPLC water and 1X PBS. The correlation is used to estimate size of the particles in the intensity graphs.

Since the PMMA-g-J10%+PB complex generally indicates the most optimal size and zeta potential and overall stability over long periods, it is used as the main graft density polymer for continued characterization and release study experiments.

For PMMA-g-J10%+CLP4 and 7 solutions, sizes are also of desired nanometer range (<200 nm) and zeta potentials correspond with the cationic CLPs increasing the ZP value from the anionic PMMA (backbone) and graft PMMA (PS). The size and ZP results are summarized in Table 4.

Sample	Zeta Potential (mV)	Particle Size (nm)
PMMA	-2.6 ± 0.9	12 ± 1
PS	-2.3 ± 1.4	48 ± 1
PMMAgJ10%-CLP4	20 ± 1	156 ± 27
PMMAgJ10%-CLP7	19 ± 1	140 ± 9

Table 4: Summary of PMMAgJ10%-CLP zeta potential and size.

Surface Properties: Figure 6 shows the surface tension measured at selected molar concentrations of grafted and un-grafted polymers. The surfactant concentration dependence of surface tension (from left to right: slow decrease and then plateau) is expected to exhibit a gradual decrease followed by an abrupt plateau. Such behavior is indicative first of the interfacial activity of free molecules then of micelle formation, which occurs at the critical micelle concentration (CMC). Since there were insufficient amounts of PMMA polymer at each graft density to get a high enough concentration stock solution at the needed volume per sample, PPAA-g-1%J (synthesized by Polysciences) and PMMA were used as a substitute to investigate block copolymer surface activity. Tween-20 and Triton X-100 are standard surfactants used to establish a baseline for finding the CMC. All solutions were made from dilutions of a high-concentration stock solution and surface tension values obtained were measured at room temperature in triplicate and averaged.

Surface tension of water averaged 72 dyne/cm. Although the polymer solutions and Jeffamine M-2070 exhibit decreasing surface tension with increase molar concentrations, only the standard surfactants Tween 20 and Triton X-100 displayed a distinct plateau. Jeffamine M-2070 exhibits behavior where surface tension decreases slowly at concentrations up to 10^{-3} M and then more rapidly at higher concentrations,

opposite to the behavior which tends to be observed. PMMA (un-grafted) alone does not appear to have significant surface activity.

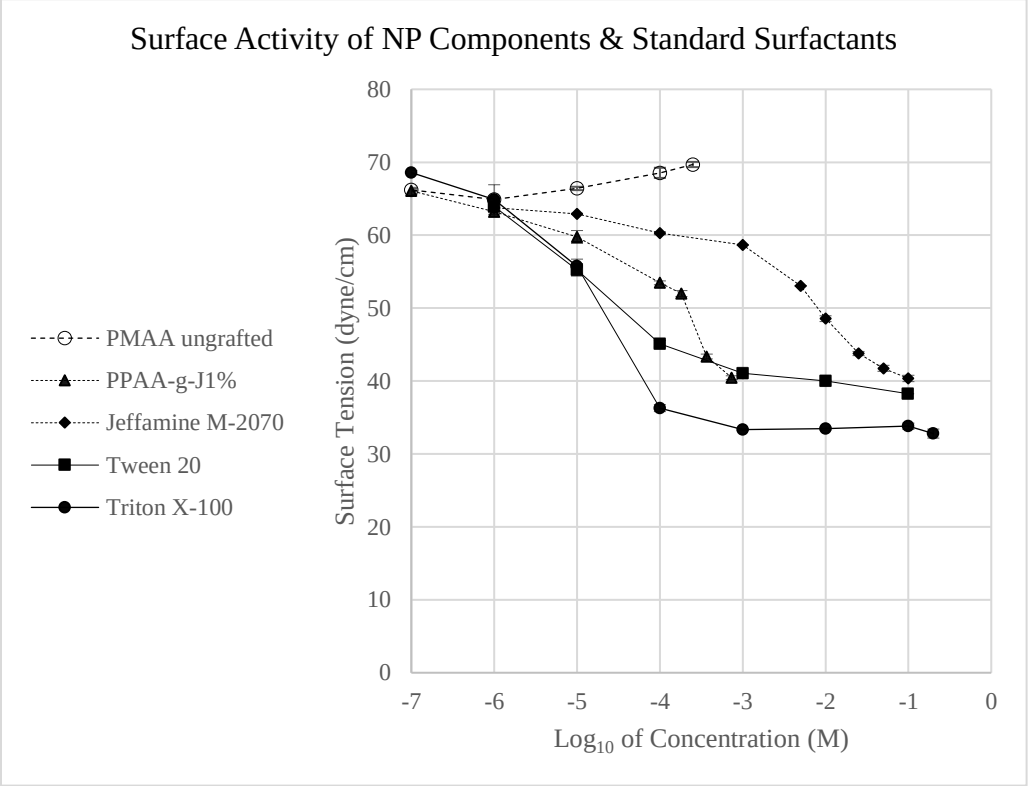

Figure 6: Surface tensions of selected polymers and surfactant solutions in dyne/cm measured with Dunouy ring surface balance methods. The logarithm of molar concentrations (mol/L) were plotted against the surface tensions (dyne/cm). Molar concentrations are of the polymer. (N=3).

Since there were limited quantities of PMMA-g-Jx% polymer solutions (without PB), only low molar dilution samples were prepared, and average surface tension values are summarized in Table 5 below. What can be observed is that surface activity in each graft polymer may be dependent on graft density of the Jeffamine, as the Jeffamine itself has surface properties at higher concentrations, as seen in Figure 6 above. The 10% grafted solution seems to lower surface tension more at the same concentration as 5% and 1% grafted solutions.

	Surface Tension (dyne/cm)		
Log of Concentration (M)	PMMAgJ1%	PMMAgJ5%	PMMAgJ10%
-5	-	-	62.4 ± 0.6
-6	64.2 ± 0.7	63.0 ± 0.3	61.7 ± 0.3
-7	71.9 ± 0.2	68.8 ± 1.3	63.8 ± 0.3
-8	72.7 ± 0.2	71.4 ± 0.2	71.9 ± 0.3

Table 5: Surface activity of low concentration PS solutions without peptides.

Rheological Properties: Shear viscosity (Pa s) was determined at set shear rates (s^{-1}) using a linear shear rate ramp at 20^{o}C automated by the Malvern Kinexus Rheometer. All measurements were taken with the same parameters indicated in the Materials & Methods.

To compare viscosity changes in PB only hydrogels and PMMA-g-J10%+PB hydrogels, 3% HEC and 3% CMC hydrogels were made for each. It is observed in both hydrogel types that the polymer-peptide hydrogels are reduced in viscosity by approximately half when compared to the PB only hydrogels. Both show similar shear thinning behavior, despite the CMC hydrogels having higher shear viscosities at the same shear rates than the HEC hydrogels (Figure 7 A and B). Similar behavior was also observed for 5% HEC and CMC hydrogels in Figure 8 A and B and shear viscosities are comparable in the 2% HEC hydrogels made from PS-PB and PS-CLP4 in Figure 9.

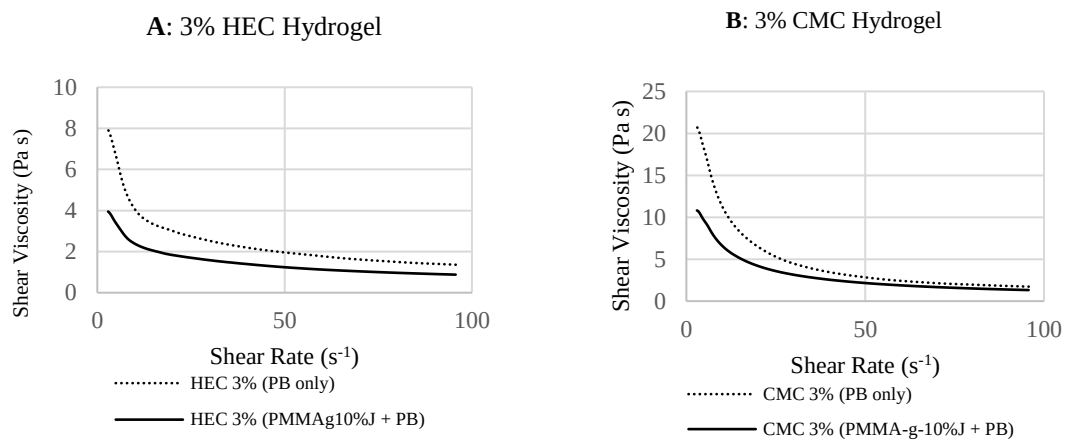

Figure 7: A – 3% HEC hydrogel formulated with 4.25 mg/mL PB only and PMMA-g-J10%+PB; **B** – 3% CMC hydrogel formulated with 4.25 mg/mL PB only and PMMA-g-10%J+PB. Live data results are plotted.

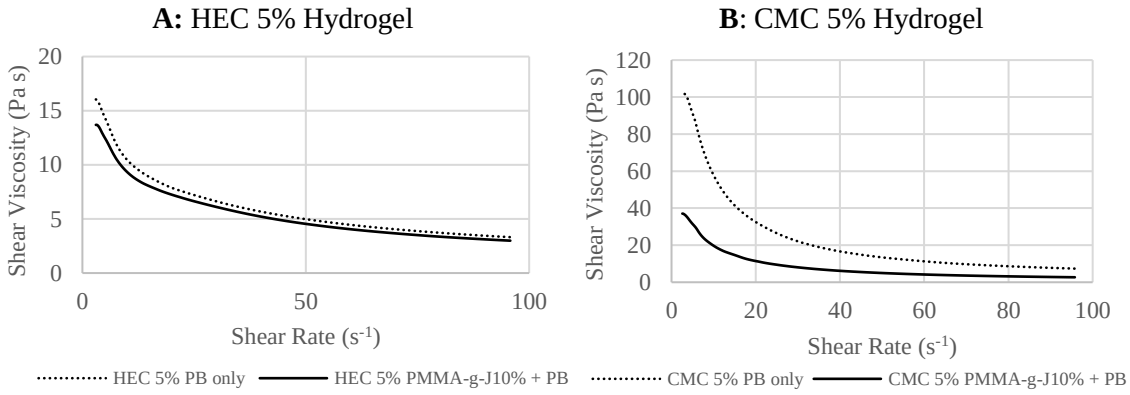

Figure 8: A – HEC 5% hydrogel formulations of PB only and PS-PB solution; **B** – CMC 5% hydrogel formulations with PB only and PS-PB solution. Live data results are plotted.

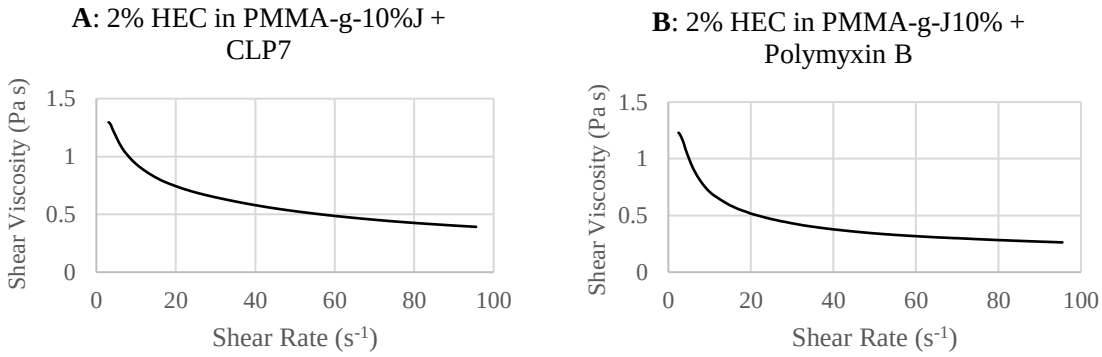

Figure 9: A – 2% HEC formulated with PMMA-g-J10%+ CLP7; B – 2% HEC formulated with PMMA-g-J10%+PB. Live data results are plotted.

Controlled Release: Results of the equilibrium membrane dialysis of PS-polymyxin B from aqueous solutions and HEC hydrogel solutions are shown in Figure 10. We can observe that there is a rapid release of PB in the first few time points (<20 hours) and then gradual slow release in the next hours. This behavior is present for both hydrogel and aqueous solutions, with slightly less cumulative release of PB in the hydrogel formulation. PB release in these formulations was fitted with 4 release kinetic models plotted in Figure 11. For the PB release, it appears that the release kinetics are best fit with the Korsmeyer-Peppas model, with an R^2 value of 0.847 for 2% HEC hydrogel and 0.978 for the aqueous solution in Figure 11 D.

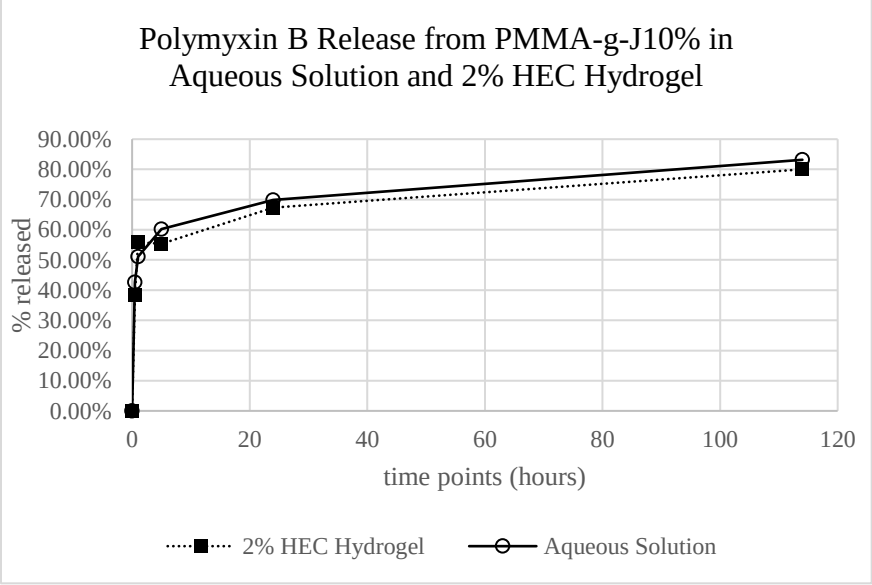

Figure 10: PB release from GP-PB in 2% HEC hydrogel and from aqueous PS-PB solution (N=1).

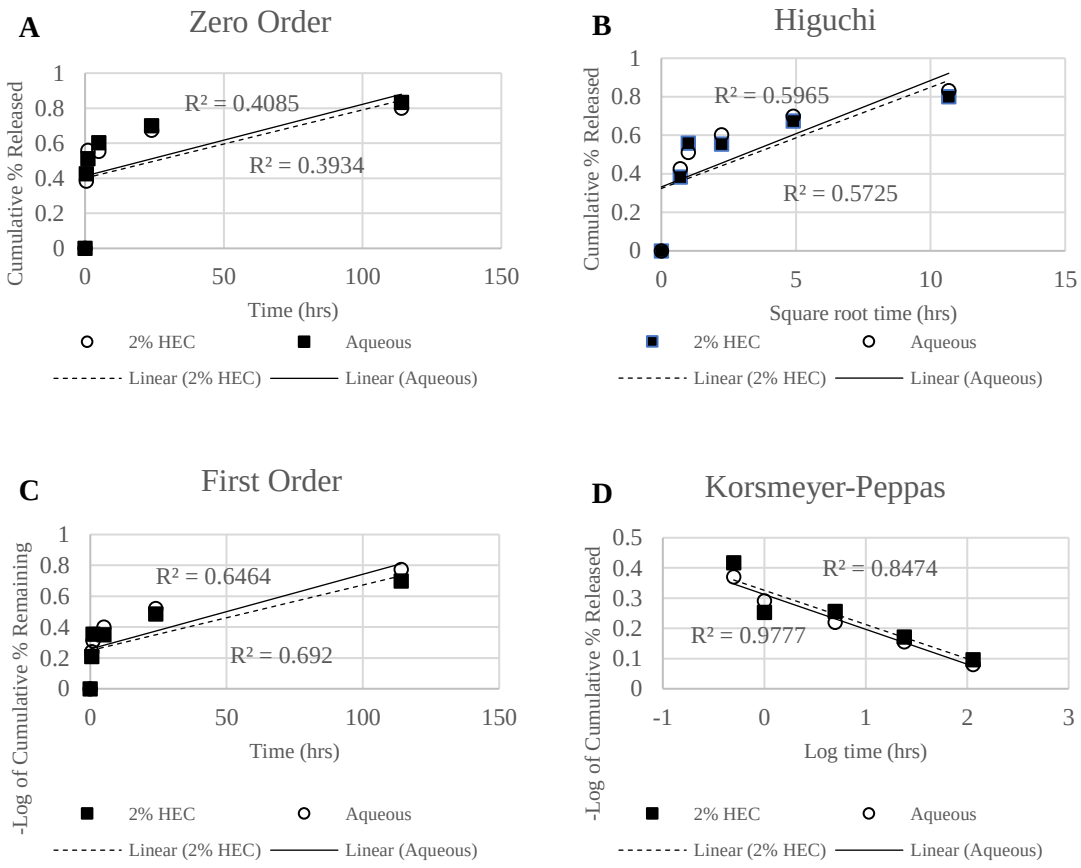

Figure 11: PB release from hydrogel and aqueous solutions modeled by zero order (A), first order (C), Higuchi (B), and Korsmeyer-Peppas (D) kinetic models.

Similarly, equilibrium membrane dialysis was performed to show release of CLP7 and GP-CLP7 dispersions from HEC 2% formulated hydrogels (Figure 12). Here, the CLP7 only hydrogel was used as a control. There is reduced rate of release of CLP7 from GP-CLP7 hydrogel when compared to the CLP7 hydrogel; this release behavior aligns with previous peptide release from aqueous solutions, where more peptide is released when compared to GP-peptide. Rapid release of CLP7 is in the first hours (<24 hours) is also observed. Rapid and near complete release of peptide is desired for this release study

as the porcine wound study requires hydrogel treatments to be changed every 24 hours and therefore needs most drug to be delivered in that time frame. CLP7 release data was also fitted by 4 release kinetic models in Figure 13. Again, the Korsmeyer-Peppas model best fits the data in comparison to the other models with $R^2 = 0.950$ for the CLP7 only hydrogel and $R^2 = 0.801$ for the GP-CLP7 hydrogel in Figure 13 D.

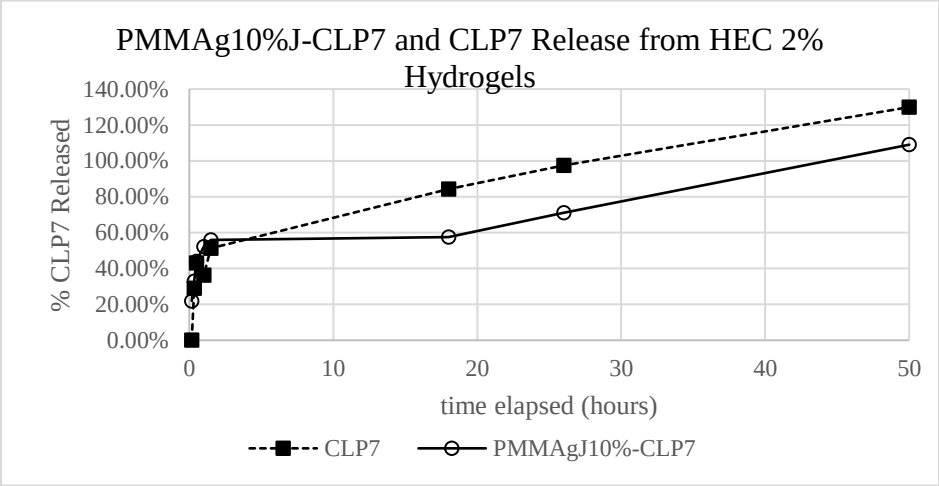

Figure 12: Release of CLP7 from 2% HEC hydrogel and GP-CLP7 2% HEC hydrogel (N=1).

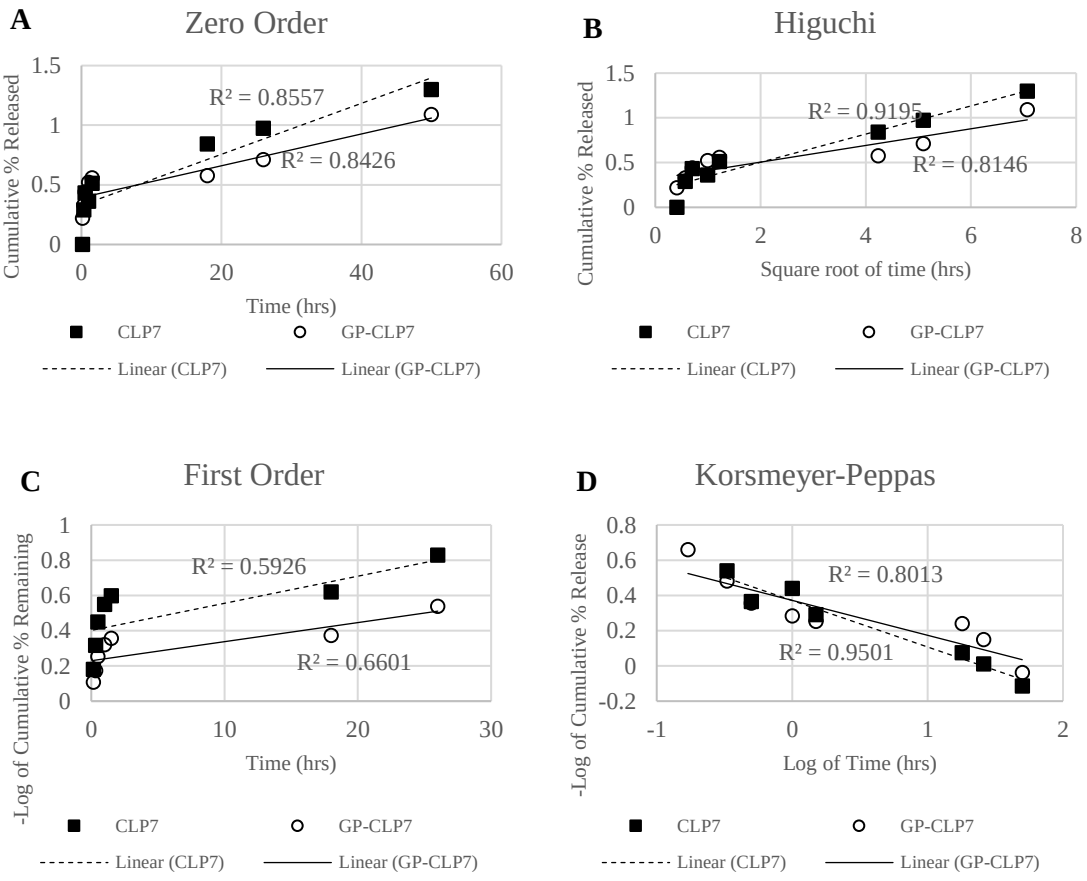

Figure 13: CLP7 release from 2% HEC hydrogel modeled by zero order (A), first order (C), Higuchi (B), and Korsmeyer-Peppas (D) kinetic models.

Antimicrobial Activity: Activity is retained by PS-PB complexes as summarized in Table 6 below for gram negative *P. aeruginosa*. PB is considered effective only against gram-negative bacteria as high concentrations are needed to kill gram-positive strains. In Figure 14 A-B, a 24-hour biofilm eradication study was conducted for Klebsiella pneumoniae (ATCC 700603). We can see that PB activity was retained in the PS-PB treatments and that PS solutions alone were not as effective. Tables 7 and 8 summarize the MICs and MBECs respectively for CLPs on select MRSA strains. Vancomycin was used in some instances as a positive control. Antimicrobial activity of CLP cationic lipopeptides was retained following complexation into nanocomplexes, and the MIC and MBEC values are consistent with those in previous work [25]

Treatment	***P. aeruginosa* (ATCC 15692, G-) MIC (µg/mL)**	***S.aureus* (ATCC 49230, G+) MIC (µg/mL)**	**MRSA 252 (G+) MIC (µg/mL)**
PB	2.5	500	125
PMMA-g-J1%+PB	2.65625	-	-
PMMA-g-J5%+PB	5.3125	-	-
PMMA-g-J10%+PB	5.3125	-	-

Table 6: MICs of PB and PMMA-g-Jx%+PB on gram-negative and gram-positive bacteria.

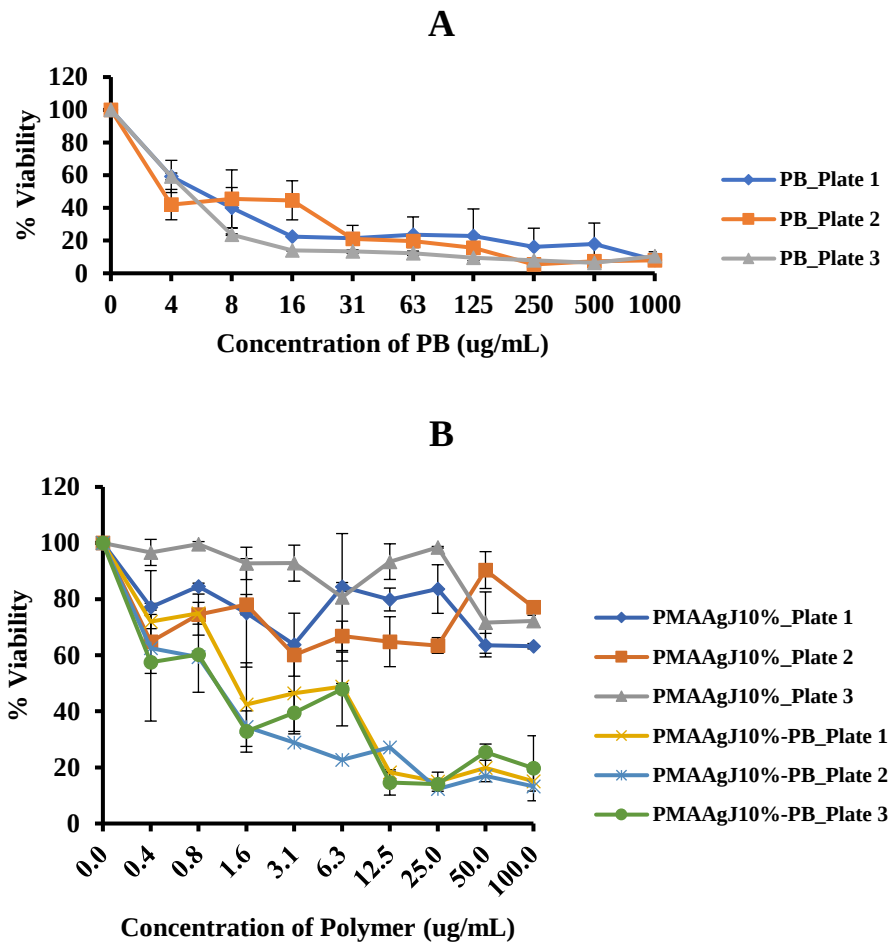

Figure 14: A, B – PB and PS-PB on Klebsiella pneumonia biofilms over 24 hours indicate retained activity of PB in graft polymer complexes.

Treatment	**MRSA 252 (G+) MIC (µg/mL)**	**MRSA USA300 (G+) MIC (µg/mL)**
PS	>200	>200
CLP4	6.25	12.5
CLP7	12.5	25
PMMAgJ10%-CLP4	12.5	25
PMMAgJ10%-CLP7	25	25
Vancomycin	0.8	12.5

Table 7: MICs of CLP's 4 and 7 alone and complexed with PS against gram positive MRSA strains. Vancomycin was used as a control.

Treatment	**MRSA 252 MBEC (μg/mL)**	**MRSA USA300 MBEC (μg/mL)**
PS	>400	>400
CLP4	12.5	12.5
CLP7	12.5	30
PMMAgJ10%-CLP4	25	12.5
PMMAgJ10%-CLP7	25	110
Vancomycin	12	50

Table 8: MBECS for MRSA strains comparing CLP4 and CLP7 alone vs. PS-CLPs. Vancomycin was used as a control.

Porcine Partial Thickness Wound study: Results for the porcine partial thickness wound study are summarized in Figure 15 below for CFU's present in samples taken from the wounds on days 2 and 5. From the results, it can be concluded that the GP-CLP7 hydrogel is more effective at reducing MRSA USA300 bacterial counts than CLP7 alone in DMSO and this behavior can be seen in both days. The control hydrogel formulation containing only GP has a slight antimicrobial effect and it should also be noted that no adverse effects on the skin were observed in both the hydrogel and DMSO solution. Although the CFU's are not reduced to the same level as the positive control, 2% mupirocin, the results are promising in that hydrogel formulation with encapsulated CLPs has an observable effect on bacteria eradication.

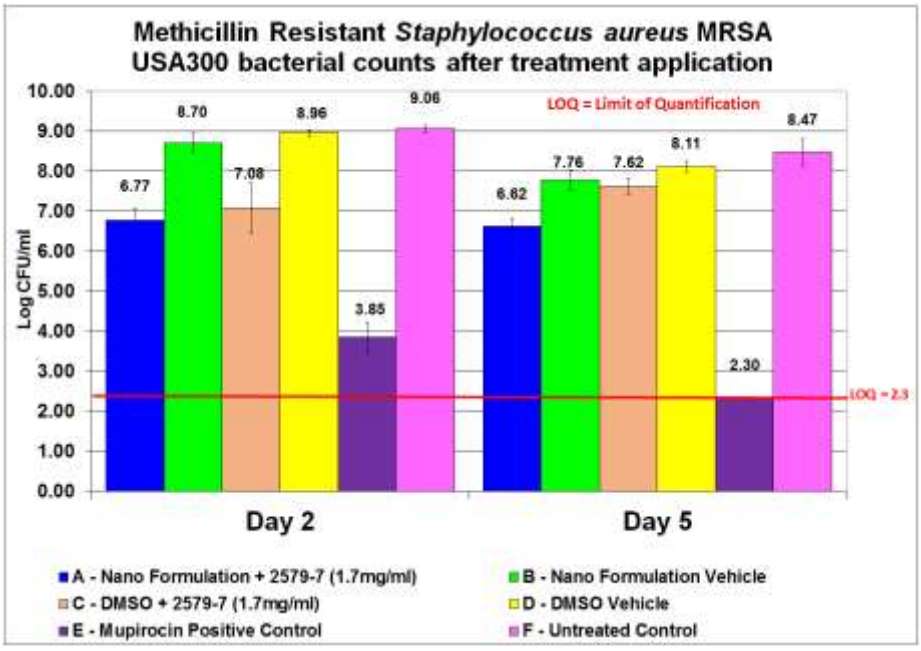

Figure 15: Porcine in-vivo wound study on wounds infected with MRSA USA300 and tested with NPs loaded with CLP7. Source: Steve Davis, University of Miami

CHAPTER 4: CONCLUSIONS & FUTURE WORK

From the methods and experiments conducted above, we can conclude that GRAPLON nanoparticles complexed with cationic peptides (PB and CLPs) show potential to be effective antimicrobial agents to eradicate bacteria in chronic wound infections. Their self-assembling nature and ability to be modified by graft density allow for a variety of polymer-peptide complexes to be tested with different charge ratios, surface properties and activity against gram positive and negative strains of bacteria. PMMA-g-J10%+PB particle sizes were shown to be generally more stable over time and have a relatively lower diameter size when compared to the other graft density polymer-PB solutions with low polydispersity. Zeta potentials of polymer-PB complexes are more positive than the anionic PS, indicating charge-charge interactions and self-assembling driven behavior. Although critical micelle concentrations were not observed in the concentration range studied, graft polymer solutions and Jeffamine M-2070 alone did show presence of some surface activity. Shear viscosities determined from variable HEC and CMC percentage composition in the PS-PB solutions demonstrated that the viscosities of hydrogels can be tunable and that shear thinning behavior was present. PB and CLPs were released from the hydrogels in a controlled manner. In vitro bacteria studies indicated that antimicrobial activity is retained in the PS-PB and PS-CLP complexes, which are affective against their respective gram-positive and gram-negative bacteria strains. A pilot porcine partial thickness in-vivo wound study showed that PS-CLP is more effective than the CLP alone in treating MRSA infected wounds, although it is not as effective as the positive control mupirocin.

For future work, more comprehensive characterization of physical properties can be used to understand better structure-function trends. This can include surface activity (critical micelle concentrations) and proper size and zeta potentials based on different charge ratios and other peptides. A more comprehensive stability study can be conducted to determine the stability/shelf life of polymers and resulting complexes over specific time periods, temperature and stress conditions. Hydrogel work can be further refined by testing a range of hydrogel concentrations, observing cross-linking behavior in different gel types and test the effects of heating or cooling on them for stability. Controlled release of peptides from hydrogels of different weight compositions can also be studied. MIC/MBEC assays can be performed with hydrogel formulations along with aqueous solutions and a more concentrated PS-CLP formulation can be developed in the case of another in-vivo wound study.

Beyond refining the tests conducted, evaluating potential cytotoxic effects on skin cells (such as human dermal fibroblasts) of the hydrogels, especially at higher nanoparticle concentrations, is an important factor to consider especially since the product will be interacting with such cells in a wound. Other studies have tested for loading or encapsulation efficiency of peptides onto nanoparticles, which can quantify the ability of the polymer to bind to the peptides [35] and their degradation rates in in-vitro conditions [36]. In-vivo studies can be expanded to treatment of burn wounds or even internal infections such as that in cystic fibrosis [37]. In such cases, the nanoparticle aqueous formulation can even be aerosolized to become another means of delivery. Alternatively, a patch instead of a topical or injectable hydrogel; the delivery system can be altered in numerous ways, as can the nanoparticle formulations themselves. Overall,

this nanoparticle-hydrogel system demonstrates good potential in becoming a viable treatment option and its combination of different aspects of drug delivery methods and solutions can contribute to overcoming ongoing obstacles in biofilm and bacterial infections.

REFERENCES

1. Gwak, J.H. and S.Y. Sohn, *Identifying the trends in wound-healing patents for successful investment strategies.* PLoS One, 2017. **12**(3): p. e0174203.
2. Han, G. and R. Ceilley, *Chronic Wound Healing: A Review of Current Management and Treatments.* Adv Ther, 2017. **34**(3): p. 599-610.
3. Lionelli, G.T. and W.T. Lawrence, *Wound dressings.* Surg Clin North Am, 2003. **83**(3): p. 617-38.
4. Xavier, J.B., et al., *Biofilm-control strategies based on enzymic disruption of the extracellular polymeric substance matrix--a modelling study.* Microbiology, 2005. **151**(Pt 12): p. 3817-32.
5. Bjarnsholt, T., *The role of bacterial biofilms in chronic infections.* APMIS Suppl, 2013(136): p. 1-51.
6. Flemming, H.C., T.R. Neu, and D.J. Wozniak, *The EPS matrix: the "house of biofilm cells".* J Bacteriol, 2007. **189**(22): p. 7945-7.
7. Soppimath, K.S., et al., *Biodegradable polymeric nanoparticles as drug delivery devices.* J Control Release, 2001. **70**(1-2): p. 1-20.
8. Dobrynin, A.V. and M. Rubinstein, *Theory of polyelectrolytes in solutions and at surfaces.* Progress in Polymer Science, 2005. **30**(11): p. 1049-1118.
9. Baraniak, B.M. and E. Waleriańczyk, *FLOCCULATION*, in *Encyclopedia of Food Sciences and Nutrition (Second Edition)*, B. Caballero, Editor. 2003, Academic Press: Oxford. p. 2531-2535.
10. Lankalapalli, S. and V.R. Kolapalli, *Polyelectrolyte Complexes: A Review of their Applicability in Drug Delivery Technology.* Indian J Pharm Sci, 2009. **71**(5): p. 481-7.
11. Gardlund, L., L. Wagberg, and M. Norgren, *New insights into the structure of polyelectrolyte complexes.* J Colloid Interface Sci, 2007. **312**(2): p. 237-46.
12. Blanco, E., H. Shen, and M. Ferrari, *Principles of nanoparticle design for overcoming biological barriers to drug delivery.* Nat Biotechnol, 2015. **33**(9): p. 941-51.
13. Bourganis, V., et al., *Polyelectrolyte complexes as prospective carriers for the oral delivery of protein therapeutics.* Eur J Pharm Biopharm, 2017. **111**: p. 44-60.
14. Jeong, Y., et al., *Polypeptide-based polyelectrolyte complexes overcoming the biological barriers of oral insulin delivery.* Journal of Industrial and Engineering Chemistry, 2017. **48**: p. 79-87.
15. Gao, Q., et al., *Rationally designed dual functional block copolymers for bottlebrush-like coatings: In vitro and in vivo antimicrobial, antibiofilm, and antifouling properties.* Acta Biomaterialia, 2017. **51**: p. 112-124.
16. Almaaytah, A., et al., *Development of novel ultrashort antimicrobial peptide nanoparticles with potent antimicrobial and antibiofilm activities against multidrug-resistant bacteria.* Drug Des Devel Ther, 2017. **11**: p. 3159-3170.
17. Hoffman, A.S., *Hydrogels for biomedical applications.* Adv Drug Deliv Rev, 2002. **54**(1): p. 3-12.
18. Veiga, A.S. and J.P. Schneider, *Antimicrobial hydrogels for the treatment of infection.* Biopolymers, 2013. **100**(6): p. 637-44.

19. Koehler, J., F.P. Brandl, and A.M. Goepferich, *Hydrogel wound dressings for bioactive treatment of acute and chronic wounds.* European Polymer Journal, 2018. **100**: p. 1-11.
20. Sosnik, A. and P.K. Seremeta, *Polymeric Hydrogels as Technology Platform for Drug Delivery Applications.* Gels, 2017. **3**(3).
21. Hamidi, M., A. Azadi, and P. Rafiei, *Hydrogel nanoparticles in drug delivery.* Advanced Drug Delivery Reviews, 2008. **60**(15): p. 1638-1649.
22. St'astny, M., et al., *HPMA-hydrogels containing cytostatic drugs. Kinetics of the drug release and in vivo efficacy.* J Control Release, 2002. **81**(1-2): p. 101-11.
23. Wen, X., et al., *Preparation of CMC/HEC Crosslinked Hydrogels for Drug Delivery*. Vol. 10. 2015.
24. Mishra, S., et al., *Delivery of siRNA silencing Runx2 using a multifunctional polymer-lipid nanoparticle inhibits osteogenesis in a cell culture model of heterotopic ossification.* Integr Biol (Camb), 2012. **4**(12): p. 1498-507.
25. Niece, K.L., A.D. Vaughan, and D.I. Devore, *Graft copolymer polyelectrolyte complexes for delivery of cationic antimicrobial peptides.* J Biomed Mater Res A, 2013. **101**(9): p. 2548-58.
26. Brown, P. and M.J. Dawson, *A perspective on the next generation of antibacterial agents derived by manipulation of natural products.* Prog Med Chem, 2015. **54**: p. 135-84.
27. Beadie, G., et al., *Refractive index measurements of poly(methyl methacrylate) (PMMA) from 0.4–1.6 μm.* Applied Optics, 2015. **54**(31): p. F139-F143.
28. Stetefeld, J., S.A. McKenna, and T.R. Patel, *Dynamic light scattering: a practical guide and applications in biomedical sciences.* Biophysical reviews, 2016. **8**(4): p. 409-427.
29. Owens, D.E., 3rd and N.A. Peppas, *Opsonization, biodistribution, and pharmacokinetics of polymeric nanoparticles.* Int J Pharm, 2006. **307**(1): p. 93-102.
30. Dash, S., et al., *Kinetic modeling on drug release from controlled drug delivery systems.* Acta Pol Pharm, 2010. **67**(3): p. 217-23.
31. Bhandari, J., et al., *Cellulose nanofiber aerogel as a promising biomaterial for customized oral drug delivery.* International journal of nanomedicine, 2017. **12**: p. 2021-2031.
32. Pastar, I., et al., *Interactions of methicillin resistant Staphylococcus aureus USA300 and Pseudomonas aeruginosa in polymicrobial wound infection.* PLoS One, 2013. **8**(2): p. e56846.
33. Bionda, N., et al., *In vitro and in vivo activities of novel cyclic lipopeptides against staphylococcal biofilms.* Protein Pept Lett, 2014. **21**(4): p. 352-6.
34. Mattison, K., A. Morfesis, and M. Kaszuba, *A Primer on Particle Sizing Using Dynamic Light Scattering*. Vol. 21. 2003.
35. Young, D.A., et al., *Design and characterization of hydrogel nanoparticles with tunable network characteristics for sustained release of a VEGF-mimetic peptide.* Biomaterials Science, 2017. **5**(10): p. 2079-2092.

36. Peng, K.-T., et al., *Treatment of osteomyelitis with teicoplanin-encapsulated biodegradable thermosensitive hydrogel nanoparticles.* Biomaterials, 2010. **31**(19): p. 5227-5236.
37. Høiby, N., *Understanding bacterial biofilms in patients with cystic fibrosis: current and innovative approaches to potential therapies.* Journal of Cystic Fibrosis, 2002. **1**(4): p. 249-254.